RSC Advances

PAPER

View Article Online
View Journal | View Issue

Cite this: *RSC Adv.*, 2015, **5**, 51290

Solvent dependent ligand transformation in a dinuclear copper(II) complex of a compartmental Mannich-base ligand: synthesis, characterization, bio-relevant catalytic promiscuity and magnetic study†

Ishani Majumder,[a] Prateeti Chakraborty,[a] Sudhanshu Das,[a] Hulya Kara,[b] Shymal Kumar Chattopadhyay,[c] Ennio Zangrando[d] and Debasis Das*[a]

An "end-off" pentadentate compartmental ligand HL has been synthesized by Mannich base condensation using *p*-cresol and 2-benzyl amino ethanol and structurally characterized. A dinuclear copper(II) complex, namely $[Cu_2(L)(\mu\text{-}OH)(H_2O)(ClO_4)_2]$, has been prepared by treating HL with $Cu(ClO_4)_2\cdot 6H_2O$ in methanolic solution with the aim of investigating its catalytic promiscuity. Single crystal structural analysis reveals that the Cu–Cu separation is 2.9 Å. Catecholase activity of the complex has been investigated in anhydrous DMSO as well as in a DMSO–water mixture with progressively increasing the quantity of water up to a 1 : 1 volume ratio in order to assess the bio compatibility of the catalyst using 3,5-DTBC as a model substrate. In anhydrous DMSO the catalytic activity reaches its peak and decreases with increasing water concentration, a feature most likely due to insolubility of 3,5-DTBQ, the product formed in the catalysis, in water. The complex also shows excellent phosphatase-like activity by exploiting the Lewis acidity, the necessary requirement for that activity, under different pH. Thorough investigation reveals that no activity is observed at pH 6 but the activity increases with increasing pH and attains a maximum at pH 9. A variable temperature magnetic study shows that the two Cu centers are antiferromagnetically coupled at low temperature with a J value of -78.63 ± 1.30 cm^{-1}. In acetonitrile medium the complex shows very exciting behavior. A new transformed ligand is generated that has been assigned as a Schiff-base ligand, 2,6-bis-[(2-hydroxy-ethylimino)-methyl]-4-methylphenol. The genesis of the new ligand is a consequence of dealkylation from HL followed by oxidation. This oxidation is counterbalanced by reduction of Cu(II) to Cu(I) as is evidenced from isolation of $[Cu(MeCN)_4](ClO_4)$ from the mixture followed by X-ray structural characterization of the species.

Received 1st April 2015
Accepted 3rd June 2015

DOI: 10.1039/c5ra05776k

www.rsc.org/advances

Introduction

Catalytic promiscuity, defined as the ability of a single active site to catalyze more than one chemical transformation, constitutes a very important property of many enzymes.[1,2] An illustrative example of this interesting feature is chymotrypsin, which exhibits catalytic promiscuity by catalyzing both amidase and phosphotriesterase reaction at its active site.[3] Many metalloenzymes containing two copper ions in their active sites can operate cooperatively.[4] Consequently di-nuclear copper complexes with two metal ions are of great interest to researchers in relation to their potential use as bimetallic catalysts, mimicking the active site of enzymes.[5,6] Only a few dinuclear copper complexes are known which may show catalytic promiscuity in important bio-relevant systems involving two important bio-relevant materials such as H_2O and O_2.[1,2] Our laboratory is actively engaged in developing the structure–function relationship in synthetic analogues of some metallobiosites like catechol oxidase, phosphatase *etc.*[5,7,8] The biocompatibility of catechol oxidase study is hampered mainly due to the insolubility and/or dissociation of the catalyst in water medium. On the other hand, it is well known that natural phosphatases accomplish the hydrolysis of the phosphate-ester bond using redox innocent Zn(II) in their active sites, employing Lewis acidity, rapid ligand exchange behavior and coordination flexibility of Zn(II).[9] To provide a breakthrough in the new arena

[a]*Department of Chemistry, University of Calcutta, 92, A. P. C. Road, Kolkata – 700009, India. E-mail: dasdebasis2001@yahoo.com*

[b]*Department of Physics, Faculty of Science and Art, Balikesir University, 10145 Balikesir, Turkey*

[c]*Department of Chemistry, IIEST Shibpur, Howrah, India*

[d]*Department of Chemical and Pharmaceutical Sciences, University of Trieste, Via L. Giorgieri 1, 34127 Trieste, Italy*

† Electronic supplementary information (ESI) available. CCDC 1053269. For ESI and crystallographic data in CIF or other electronic format see DOI: 10.1039/c5ra05776k

of catecholase activity we have synthesized a water soluble dinuclear copper(II) complex of a symmetric Mannich base ligand as a model for the *met* form of the active site of catechol oxidase. In addition to exhibit catecholase activity the complex is also able to catalyze the hydrolysis reaction of phosphate-ester bond when the substrate is 4-nitro phenyl phosphate (4-NPP). Along with the versatile catalytic activity, variable temperature magnetic study and electrochemical behavior of the complex has been investigated. More interestingly, in acetonitrilic medium a unique ligand transformation was observed, which was coupled with dealkylation and concomitant redox reaction. All these interesting features have been vividly portrayed in this manuscript.

Results and discussion

Design, rationalization, and characterization of ligand

Mannich reaction is a relevant organic reaction for C–C bond formation widely used in the synthesis of nitrogenous molecules, especially secondary and tertiary amine derivatives, and applied as a key step in the synthesis of many bioactive molecules and natural products.[10] Foremost we had aspired to the synthesis of a conventional phenolic ligand with N, N, O donor sites by this age-old reaction with maximum yield and purity. For Mannich condensation a secondary amine [2-benzyl amino ethanol] and formaldehyde on one side and an activated phenyl ring [*p*-cresol] on the other side are generally chosen for the occurrence of aromatic electrophilic substitution reaction. The interaction between formaldehyde and 2-benzyl amino ethanol first of all generates methylene iminium intermediate which subsequently attacks *p*-cresol at two *ortho* positions (with respect to phenolic –OH) and thereby generates an end-off compartmental ligand, HL, having N_2O_3 donor set (Fig. 1). Since some amount of the intermediate (methylene iminium) still remains in the equilibrium of the reaction, column chromatographic separation is required to obtain the pure ligand.

Synthesis, rationalization, and characterization of the metal-complex

The complex was synthesized adopting sequential or stepwise synthesis technique *i.e.* the Mannich-base ligand HL was synthesized and characterized first, then it was treated with a methanolic solution of copper(II) perchlorate dihydrate. Complex **1** was obtained after recrystallization of the product obtained from the above reaction in ethanol medium. The IR spectrum of the complex shows a band due to C–N stretch at 1576 cm^{-1} and skeletal vibration at 1496 cm^{-1}. Broad band centered at 1078 cm^{-1} indicates the presence of perchlorate ion in the complex.[11] Additionally, the observed bands at 1132, 1281, 897 cm^{-1} confirm the presence of bridging perchlorate ion in the complex.[11]

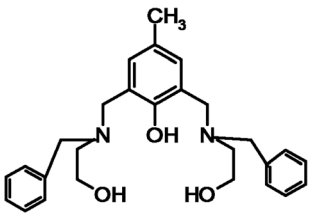

Fig. 1 Designed ligand with N_2O_3 donor sets obtained by proper tuning of the Mannich reaction.

Solution studies: electronic spectra, potentiometric titration and mass spectrometry

In order to characterize the catalytically relevant species for hydrolase like activity UV-Vis study, potentiometric titration and ESI-MS study are carried out in DMSO–water mixtures (3 : 1). Electronic spectral study of the complex **1** was performed at different pH (Fig. S7†). The band around (600–650) nm composed of d–d transition changes significantly and thus suggests that the coordination environment around the Cu(II) centers must be considerably distinct at different pH.

By examining the electronic spectrum of **1** as a function of pH an interesting spectral change that involves the species in equilibrium could be observed. At very lower pH ~ (3–4) the potentiometric titration indicates the pK_a which corresponds to the deprotonation of phenolic –OH (Fig. S8; Table S1†)) and the phenoxo ligand thus obtained helps to generate the dinuclear species as **1a** $[Cu_2L(H_2O)_2]^{3+}$. When the pH of the solution is raised to 5 another protonation–deprotonation equilibrium is observed involving one of the coordinated H_2O, with corresponding pK_a of 6.1 (Table S1†) and the species is most like to be $[Cu_2L(\mu\text{-}OH)(H_2O)]^{2+}$ (**1b**) (Fig. 2.) The second pK_a is calculated as 8.15 and it can be attributed to the formation of $[Cu_2L(\mu\text{-}OH)(OH)]^{+}$ (**1c**) by deprotonation of the bound water molecule from the species **1b**. All this protonation–deprotonation phenomena is depicted in the Scheme 1.

From the above discussion it is clear that at nearly neutral pH our complex should exists as **1b** and that very proposition is supported by ESI-MS study of complex **1** (Fig. S9†) in DMSO–water medium (pH = 6.7) where we observed the base peak at ~297.78 amu (calc. 297.71 amu) matches well with the *m*/*z* value of $[Cu_2L(\mu\text{-}OH)(H_2O)]^{2+}$ (**1b**).

Crystal structure description

The ORTEP diagram of complex **1** with atom numbering scheme is depicted in Fig. 3, and a selection of bond lengths and angles is given in Table 1. The crystal structure reveals that in the dinuclear complex the copper atoms Cu1 and Cu2 possess a distorted square pyramidal and octahedral geometry, respectively. The doubly bridging phenoxo and hydroxo oxygen atoms occupy the basal plane, and the metals complete their coordination geometry through the amine–nitrogen and hydroxy–oxygen donors of the pentadentate chelating ligand.

In the basal plane the Cu–O bond distances are comparable in lengths ranging from 1.912(6) to 1.963(7) Å (Table 1), the shorter values for the hydroxo oxygen O1. On the other hand the Cu–N (amino) bond distances are slightly longer, of 2.004(8) and 1.988(8) Å. The bridging bond angles subtended by the phenoxo and hydroxo groups, of Cu1–O1–Cu2 and Cu1–O4–Cu2 of 99.7(3) and 97.1(3)°, respectively, lead to a metal–metal

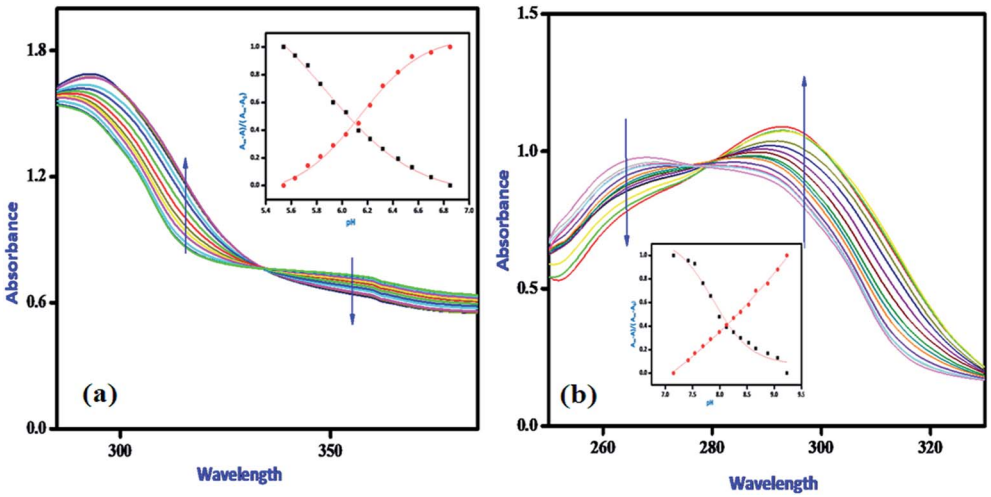

Fig. 2 Spectrophotometric titration of **1** (a) (pH value: 5.54–6.85; pK_a = 6.10) and (b) (pH value: 7.15–9.23; pK_a = 8.15) conditions: complex = 10^{-3} [M]; [KCl] = 0.100 mol L^{-1}; [KOH] = 0.100 mol L^{-1}; in solution DMSO–water (75 : 25% v/v; 50 mL) at 25 °C.

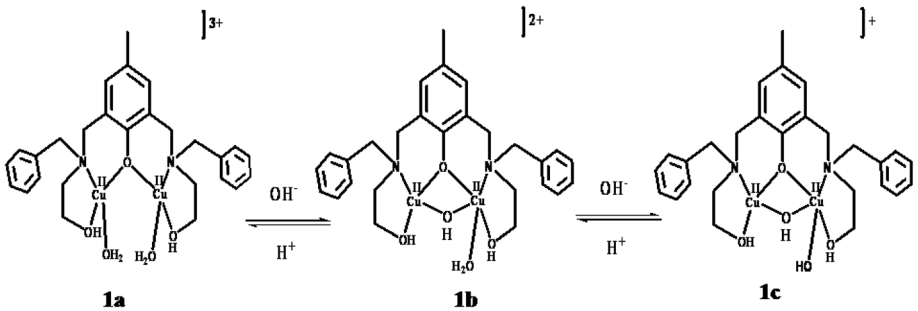

Scheme 1 Structural representation of the pH-dependent aqueous equilibria of **1**.

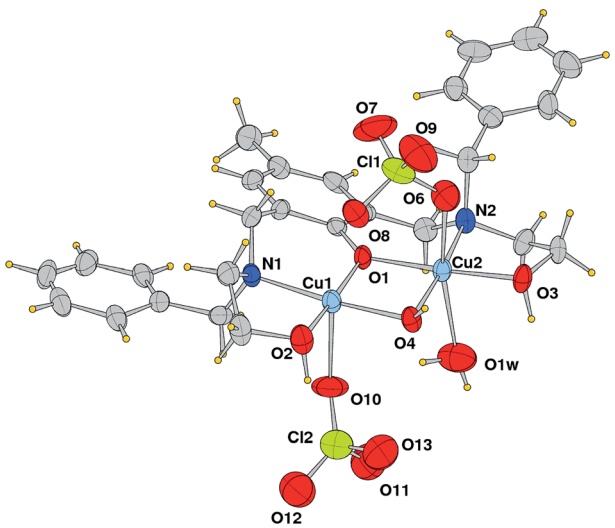

Fig. 3 ORTEP drawing (ellipsoid probability 30%) of complex **1** (C atoms not labelled for sake of clarity).

Table 1 Selected coordination bond lengths (Å) and angles (deg) for complex **1** with esds in parentheses

Cu1–O1	1.916(7)	Cu2–O1	1.912(6)
Cu1–O2	1.962(8)	Cu2–O3	1.924(7)
Cu1–O4	1.940(7)	Cu2–O4	1.963(7)
Cu1–N1	2.004(8)	Cu2–N2	1.988(8)
Cu1–O10	2.561(11)	Cu2–O1w	2.519(12)
Cu1···Cu2	2.926(2)	Cu2–O6	2.590(10)
O1–Cu1–O4	81.7(3)	O1–Cu2–N2	93.2(3)
O1–Cu1–O2	174.0(4)	O3–Cu2–N2	85.5(3)
O4–Cu1–O2	97.5(3)	O4–Cu2–N2	174.1(3)
O1–Cu1–N1	94.7(3)	O1–Cu2–O1w	100.2(4)
O4–Cu1–N1	174.9(3)	O3–Cu2–O1w	82.9(4)
O2–Cu1–N1	85.6(3)	O4–Cu2–O1w	88.7(3)
O1–Cu1–O10	87.8(4)	N2–Cu2–O1w	90.4(4)
O4–Cu1–O10	86.1(4)	O1–Cu2–O6	92.3(3)
O2–Cu1–O10	98.2(4)	O3–Cu2–O6	85.0(3)
N1–Cu1–O10	97.5(4)	O4–Cu2–O6	82.9(3)
O1–Cu2–O3	176.7(3)	N2–Cu2–O6	99.3(3)
O1–Cu2–O4	81.3(3)	O1w–Cu2–O6	163.8(4)
O3–Cu2–O4	100.2(3)	Cu1–O1–Cu2	99.7(3)
		Cu1–O4–Cu2	97.1(3)

separation of 2.926(2) Å. The apex of the square pyramidal geometry at Cu1 is occupied by a perchlorate oxygen (Cu1–O10 = 2.561(11)) (Å). On the other hand, the axial positions in the octahedral geometry of Cu2 are occupied by an aqua ligand and an oxygen atom of the second perchlorate as shown in Fig. 3 (Cu2–O1w = 2.519(12)); Cu2–O6 = 2.590(10) (Å). All these Cu–O

bond lengths are longer with respect to the other coordination bond distances as consequence of the Jahn–Teller effect.

The crystal packing shows the complexes paired about a crystallographic center of symmetry leading to the formation of strong H-bonds between the alcoholic groups (O4···O3′ = 2.571 Å, Fig. 4).

PXRD study of the complex 1

In order to gain a better understanding of the uniformity of the complex **1**, we performed a PXRD study (Fig. S10†) and compared the observed pattern with the PXRD pattern generated from the CIF file of the crystal. The two patterns are nearly superimposable and thereby suggests that the crystalline nature of the species remains intact in bulk form. Therefore it is reasonable to explore all the catalytic activities with this bulk.

Catecholase activity

Catechol oxidase, a type-3 copper protein can bind oxygen reversibly at room temperature and so it can be employed to oxidize phenols to respective *o*-benzoquinones. As a model of the enzyme we have taken one dinuclear hydroxo bridged complex of Cu(II) and have studied it's efficiency towards the oxidation of 3,5-di-*tert*-butylcatechol (3,5-DTBC) to 3,5-di-*tert*-butylbenzoquinone (3,5-DTBQ). Interestingly, it displays significant catalytic activity towards the oxidation of 3,5-DTBC to 3,5-DTBQ in DMSO medium. Before proceeding into detailed kinetic study we have checked the ability of the complex to mimic the active site of catechol oxidase by treating 1×10^{-4} mol dm^3 solutions of complex **1** with 1×10^{-2} mol dm^{-3} (100 equivalents) of 3,5-DTBC under aerobic condition. Fig. 5 shows the spectral change for the complex upon addition of 100-fold 3,5-DTBC (1×10^{-2} M) observed at an interval of 5 min in DMSO medium. The kinetics of the oxidation of 3,5-DTBC was determined by monitoring the increase of the concentration of the product 3,5-DTBQ and the experimental conditions were the same as we reported earlier.[7] All the complexes showed saturation kinetics and a treatment based on the Michaelis–Menten

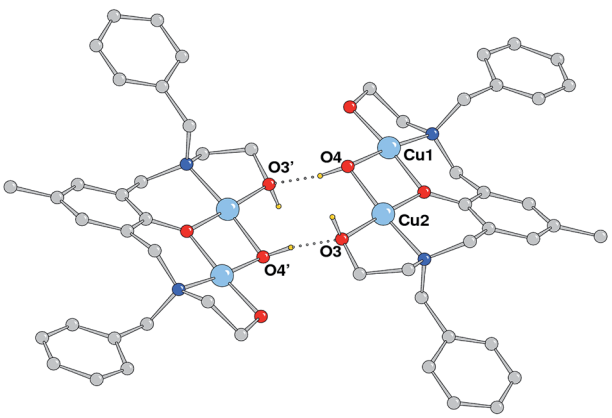

Fig. 4 Crystal packing: dinuclear complexes paired through strong hydrogen bonds involving the alcoholic groups (O4···O3′ = 2.571 Å; O4–H···O3′ = 167°). Perchlorate and water molecules are not shown for clarity.

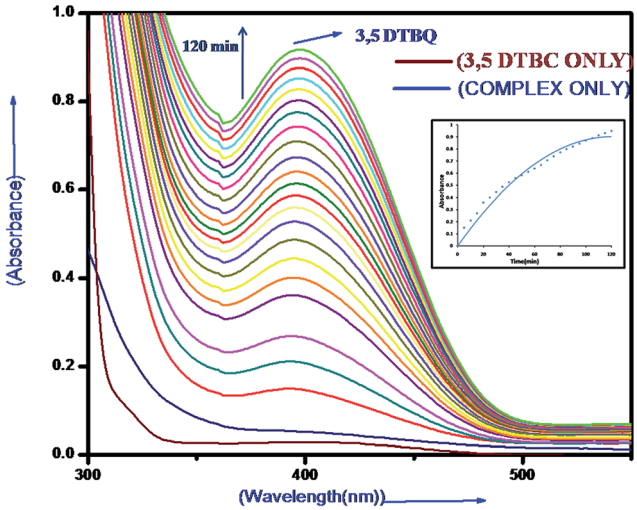

Fig. 5 Changes observed in UV-vis spectra of complex **1** for 120 minutes (conc. 1×10^{-4} M) upon addition of 100-fold 3,5-DTBC (1×10^{-2} M). (inset) Absorption profile due to the formation of 3,5-DTBQ (λ_{max} = 393 nm) on addition of 3,5-DTBC to complex **1**.

model seemed to be appropriate. The binding constant (K_M), maximum velocity (V_{max}), and rate constant for dissociation of substrates (*i.e.*, turnover number, k_{cat}) were calculated for the complex by using the Lineweaver–Burk graph of $1/V$ *vs.* $1/[S]$, using the equation $1/V = \{K_M/V_{max}\}\{1/[S]\} + 1/V_{max},\}$, and the kinetic parameters are presented in Table 2 and in S2.†

Mechanistic interpretation on catecholase activity exhibited by complex 1

The mechanistic interpretation of catecholase activity of synthetic analogues of catechol oxidase divulges that substrate–catalyst interaction is the key step of the mechanism. Catechol may bind the catalyst in a variety of coordination mode starting from monodentate asymmetric type[16] to bridging bidentate[17a] or *via* combination of both.[5,7] However in the present case the spectral study is not distinct enough to assign the binding mode of catechol to the copper center as we noticed in our earlier studies.[5,7] However, a pre-equilibrium of the free complex and the substrate exists preceding to the intramolecular electron transfer in the key step of the mechanism followed by reduction of Cu(II) to Cu(I) with concomitant oxidation of catechol to quinone. Now the rate determining step of the mechanism may be either the re-oxidation of Cu(I) by dioxygen or the intramolecular electron transfer. Since in our case the d–d band remains intact with slight blue shift (Fig. S11†) during the catalytic reaction, and the detection of the intermediate by mass spectral study after one hour of the mixing (Fig. S12†) supports the fact that the intramolecular electron transfer is most probably the rate determining step. In the catalytic cycle the role of dioxygen is very crucial for regeneration of the catalyst with its concomitant reduction of either kind: (i) two electron reduction to H_2O_2 or (ii) four electron reduction to water.[16,17] But in our case the spectral study after treatment with iodide fails to detect I^{3-} (Fig. S13†) and thereby clearly excludes the possibility of dioxygen reduction to H_2O_2 (Fig. 6 and 7).

Table 2 First order rate constants for the oxidation of catechols by the complex **1** and the previously reported analogous dinuclear Cu(II) complexes using 3,5-DTBC as substrate

Complex	Solvent	Cu···Cu (Å)	k_{cat} in h^{-1}	Ref.
$[Cu_2(L)(\mu\text{-}OH)(H_2O)(ClO_4)_2]$	DMSO	2.926	0.76×10^2	Present work
$[Cu_2(H_2bbppnol)(\mu\text{-}OAc)(H_2O)_2]Cl_2 \cdot 2H_2O$	MeOH	3.400	0.28×10^2	12
$[Cu_2(H_2btppnol)(\mu\text{-}OAc)](ClO_4)_2$	MeOH	3.400	0.28×10^2	12
$[Cu_2(L1)(\mu\text{-}OAc)](ClO_4)_2 \cdot (CH_3)_2CHOH$	MeOH	3.350	0.90×10^2	2
$[Cu_2(L2)(\mu\text{-}OAc)](ClO_4) \cdot H_2O \cdot (CH_3)_2CHOH$	MeOH	3.560	1.83×10^2	2
$[Cu_2(tppnol)(OAc)(ClO_4)_2$	MeOH	3.360	0.11×10^2	13
$[Cu_2L_{3H}(OH)]$	MeOH–water mixture	3.500	0.02×10^2	14
$[Cu_2(L_{OCH3})(\mu\text{-}OH)]^{2+}$	Acetone	2.980	0.21×10^2	15
$[Cu_2(L_{CH3})(\mu\text{-}OH)]^{2+}$	Acetone	2.966	0.10×10^2	15
$[Cu_2(L_F)(\mu\text{-}OH)]^{2+}$	Acetone	2.969	0.05×10^2	15

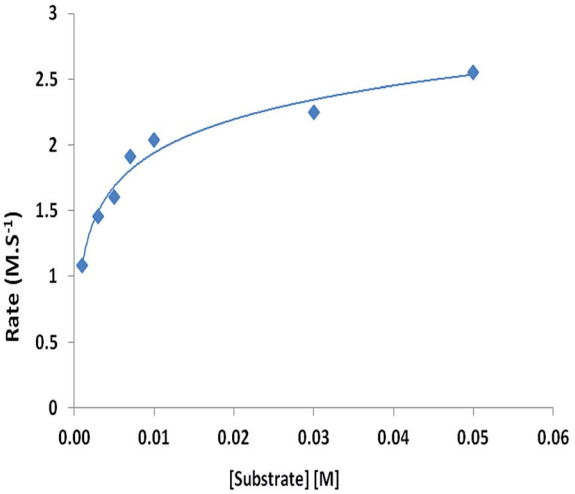

Fig. 6 Dependence of rate of reaction on substrate concentration for complex **1** (100 μM) at 25 °C in DMSO for oxidation of catechol.

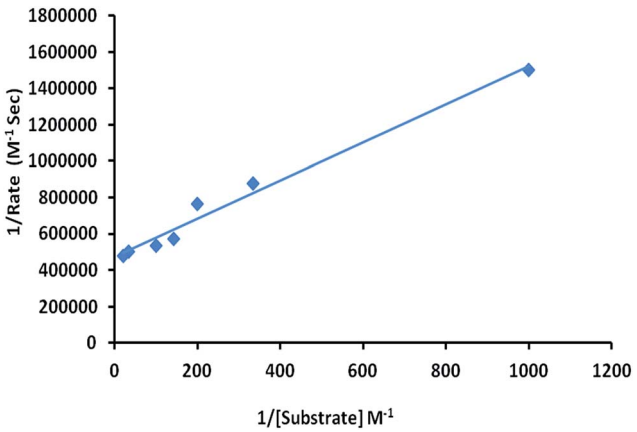

Fig. 7 Lineweaver–Burk plots for complex **1** in DMSO medium for oxidation of catechol.

Study of catecholase activity in water medium: searching for a bio-compatible catalyst

There are plenty of reports in the literature of synthetic analogues of catechol oxidase in different solvents,[7,12–18] but only few reports deal with the activity of catalyst in water medium.[14] Metal complexes of Schiff base cannot mimic catecholase activity in water medium as they have a imine bond which may get hydrolyzed in presence of water. So we have designed an ammine complex of Mannich base ligand which is soluble in water and therefore suitable to explore its bio compatibility mode. Our synthesized complex **1** shows good catalytic efficiency up to a 50 : 50 solvent mixture of DMSO : water medium (Fig. S14 and S15†). The catalytic efficiency decreases with increasing the water quantity which may be due to the precipitation of DTBQ and thereby the contribution of the increasing concentration of 3,5-DTBQ may not be assessed by spectral scan. However, at this point further extensive work is necessary to get deep insight on role of water in catecholase activity as done by other investigator.[14]

Phosphatase activity

There are plenty of literature reports in which labile coordination sites of dinuclear transition metal complexes assist the hydrolysis of phosphate esters.[8a] The criteria for the molecular species to function as an efficient catalyst towards the hydrolysis is to provide the H_2O/OH^- species as nucleophile. Since our complex possesses a nucleophile constituted by metal bridging hydroxyl group and a bound water molecule it would be reasonable to explore its phosphatase activity following the hydroxylation of 4-NPP (4-nitrophenyl phosphate salt). The catalytic efficiency of the complex was determined using the method of pseudo-first order rate constant by monitoring the growth of 4-nitrophenolate absorption band at 425 nm in 75% DMSO solution at pH 9.0 at 25 °C. The concentration of the substrate 4-NPP was always kept at least 10 times larger than that of the Cu(II) complex to maintain the pseudo-first order condition. Initially a series of solutions of substrate 4-NPP, having 5 different concentrations, were prepared from concentrated stock solution of substrate using DMSO and buffered water in 3 : 1 ratio. After the addition of substrate to the solution of the catalyst a new band corresponding to 4-nitrophenolate appeared at 425 nm. The course of this typical reaction at pH 9.0 is shown as.

The first order rate constants for catalytic phosphate ester cleavage were determined from the slopes of the plots of $\log[A_\infty/A_\infty - A_t]$ *vs.* time for different sets. In order to determine the rate dependence on the substrate concentration, the complex is

treated with different concentrations of 4-NPP. Initially a first order dependence of the substrate concentration was observed, while saturation kinetics was observed at higher concentration (Fig. 9).

The rates of reaction for various substrate concentrations were interpreted with Michaelis–Menten approach and the data fitted by means of Lineweaver–Burk plot to calculate the kinetic parameters (Fig. 10).

For correction of spontaneous cleavage of 4-NPP in presence of the buffer, each reaction was carried out against a reference cell that was identical to the sample cell in composition except for the absence of complex **1**. The time dependent spectral scan (Fig. S21†) clearly suggests that the rate of spontaneous hydrolysis of 4-NPP is negligible in absence of catalyst and hence the rate of spontaneous hydrolysis of 4-NPP is not taken into account in the kinetic measurements. To confirm that the synthesized ligands and the copper perchlorate-salt used in the reaction do not participate in the catalytic process, rigorous control experiments have been performed to intake their role if any (Fig. S22–23†). The results indicated no appreciable change as we noticed in our earlier experiments also (Table 3).[8]

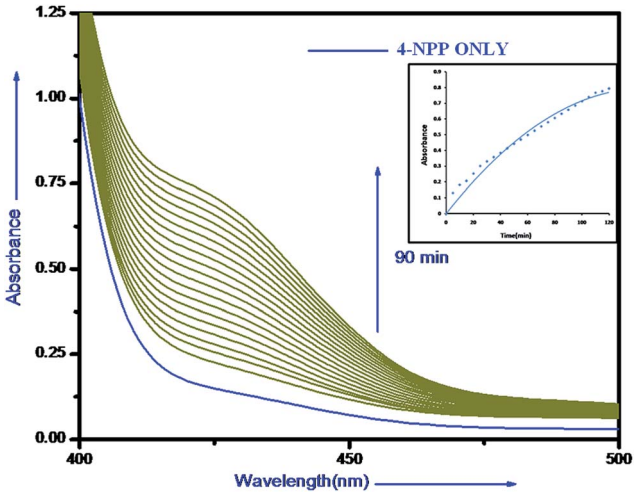

Fig. 8 Wavelength scan for the hydrolysis of 4-NPP in the absence and presence of complex **1** (substrate : catalyst = 20 : 1) in 75% DMSO-buffer medium at pH 9.0 recorded at intervals of 5 minutes for 90 minutes (pH = 7.0, T = 25 °C); [4-NPP] = 1×10^{-3}(M), [complex] = 0.05×10^{-3}(M). The arrow shows the change in absorbance with reaction time. (inset) Absorption profile due to the formation of 4-nitrophenolate (λ_{max} = 425 nm) on addition of 4-NPP to complex **1**.

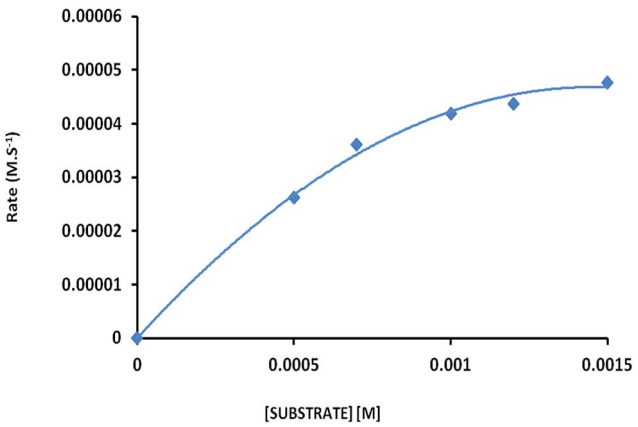

Fig. 9 Dependence of rate of reaction on substrate concentration for complex **1** (50 μM) at 25 °C in 75% DMSO (pH 9) for hydroxylation of 4-NPP.

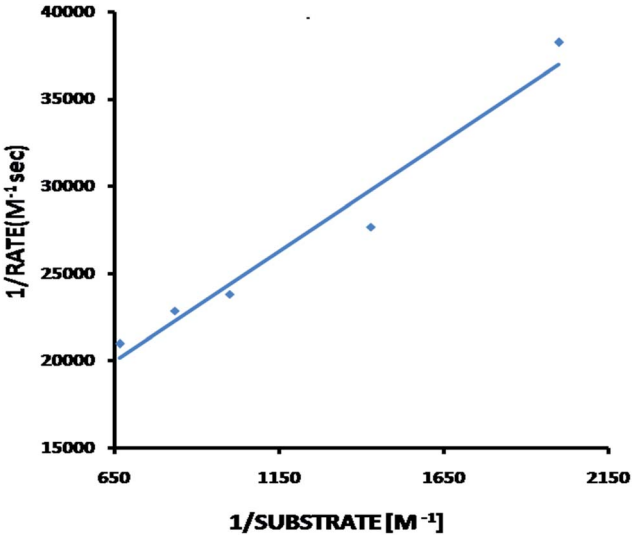

Fig. 10 Lineweaver–Burk plot for the 4-NPP hydroxylation by complex **1**.

The effect of pH on catalytic activity was also studied in the pH range 6–9 (Fig. 8 and S17–S20†). It is observed that the reaction rate increases on increasing the pH and finally gets saturated at high pH 8.5. The complex shows no activity below pH 6.5, and the activity slightly increases at pH 7.0 and becoming maximum at pH 8.5–9.0. The phosphatase activity of complex **1** is thus strongly influenced by pH of the reaction mixture and reveals sigmoidal shape profiles (Fig. 11). Here the data were fitted using a Boltzman model, resulting $pK_a = 7.8 \pm 0.2$. Which is in fair agreement with the value ($pK_a = 8.15$) found from potentiometric titration [Fig. 2(b)]. Slight difference in the value may be explained by the substrate–catalyst interaction, which in some how affects the Lewis acidity of the Cu(II) centers. Although such interpretation should be considered as speculative because no further experimental and theoretical evidence is available at present. However, deprotonation of the Cu(II) coordinated water molecule may occurs at higher pH to generate the catalytically active species $[Cu_2(L)(\mu\text{-}OH)(OH)]^+$ and consequently the rate of hydrolysis of 4-NPP increases at higher pH (>7.5). This pH-dependent rate constant suggests that deprotonation of a metal-bound water molecule favors the generation of catalytically active nucleophile.[20–23]

As far as mechanistic interpretation of phosphate-ester bond hydrolysis is concerned it may be stated that the incoming substrate first of all binds effectively to the catalyst followed by nucleophilic attack by the metal bound hydroxo group present in the complex to cleave P–O bond with subsequent release of the product in the form of 4-nitrophenolate ion.

Table 3 First-order rate constants for the hydrolysis of phosphate esters by the complex **1** and the similar previously reported Cu(II) complexes

Complex	Conditions	k_{cat} in s^{-1}	Substrate	Ref.
$[Cu_2(L)(\mu\text{-}OH)(H_2O)(ClO_4)_2]$	3 : 1 DMSO : water, pH 9.0, 25 °C	1.69	4-NPP	Present work
$[Cu_2(L1)(\mu\text{-}OAc)](ClO_4)_2\cdot(CH_3)_2CHOH$	1 : 1 MeCN : water, pH 8.0, 50 °C	2.97×10^{-4}	2-4 BDNPP	2
$[Cu_2(L2)(\mu\text{-}OAc)](ClO_4)\cdot H_2O\cdot(CH_3)_2CHOH$	1 : 1 MeCN : water, pH 8.0, 50 °C	5.16×10^{-4}	2-4 BDNPP	2
$[Cu_2L\ (Cl_3)]$	1 : 1 MeCN : water, 50 °C	5.30×10^{-4}	2-4 BDNPP	19
$[Cu_2(L)(\mu\text{-}OH)]^{2+}$	1 : 1 MeCN : water, 50 °C	2.10×10^{-2}	2-4 BDNPP	1

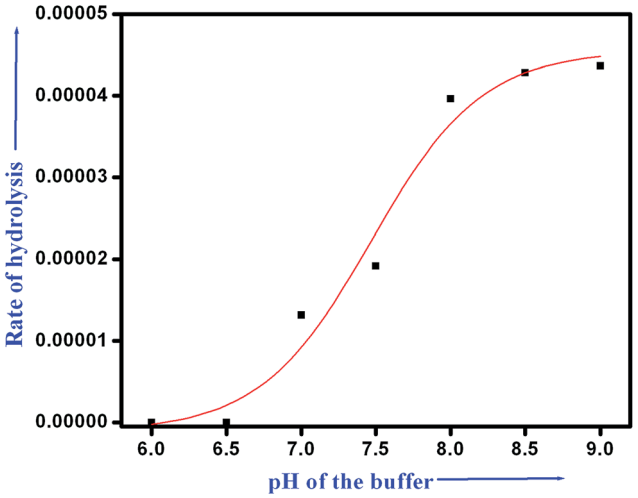

Fig. 11 Dependence of the rate of 4-NPP hydroxylation on pH by complex **1** in 75% DMSO-buffer at 25 °C.

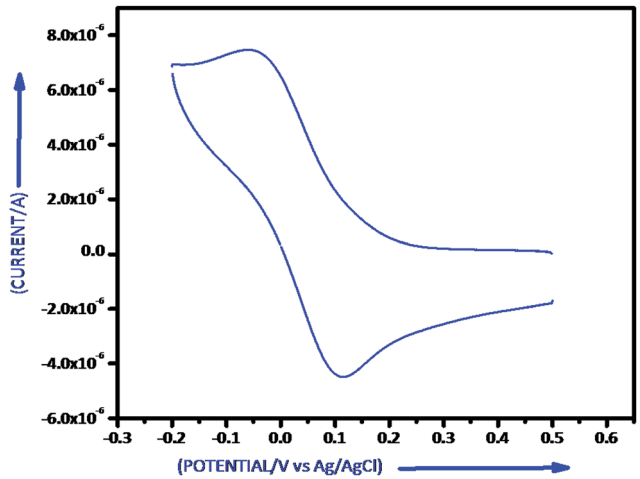

Fig. 12 CV cyclic voltammogram of complex **1**, in DMSO, at the GC electrode at 100 mV s^{-1} scan rate as representative.

Cyclic voltammetric study

In DMSO solution the complex **1** undergoes two reductive responses at E_{pc} values of −0.05 V and −0.51 V, with the later peak having current height 2.5 times that of the first peak (Fig. S28†). On reverse scan a strong stripping peak is detected at 0 V, along with an oxidative response at 0.1 V, which is probably coupled to the reductive peak at −0.05 V. On restricting the scan in the negative side up to −0.2 V a quasireversible couple is detected with $E_{1/2}$ value of 0.03 V, peak to peak separation of 172 mV and $i_{pc}/i_{pa} = 1.17$; no stripping current is observed on scan reversal in this case (Fig. 12). In differential pulse voltammetry (DPV) experiments two reductive peaks are detected at E_p = −0.064 V and −0.316 V corresponding to $E_{1/2}$ values of −0.04 V and −0.29 V respectively ($E_p = E_{1/2} - \Delta E/2$; where ΔE is the pulse amplitude which in our experiment is 0.05 V). However, in this case the first peak has almost 3.4 times the current height of the second peak. We assign the quasi-reversible reduction at 0.03 V observed in CV experiments to Cu(II)/Cu(I) reduction of one of the Cu(II) center, while the irreversible reduction at −0.5 V is assigned to the Cu(II)/Cu(0) reduction of the second center along with Cu(I)/Cu(0) reduction of the first center. Though the mixed valent Cu(I) Cu(II) species is stable in cyclic voltammetry time scale, it probably undergoes slow decomposition due to strain suffered by the relatively rigid ligand to accommodate a tetrahedral Cu(I) and another square planar Cu(II) center, and this may account for the abnormally low current height of the peak at −0.316 V in DPV. The cyclic voltammogram and differential pulse voltammogram of the complex is invariant with respect to time in DMSO solvent.

On addition of 3,5-DTBC to a DMSO solution of the complex, the Cu(II)/Cu(I) couple at 0.3 V is replaced by a new couple with E_{pc} = −0.02 V and E_{pa} = +0.3 V and the current height of the reductive peak being much larger than the metal based couples. We tentatively assign the cathodic peak at −0.02 V to the reduction of free 3,5-DTBQ to $Cu(II)_2$ bound di-deprotonated 3,5-DTBC, and the anodic peak at +0.3 V to oxidation of $Cu(II)_2$ bound 3,5-DTBC to free 3,5-DTBQ (Fig. 13).

Magnetic study

The magnetic properties of complex **1**, in the form of χ_M and $\chi_M T$ (χ_M is the susceptibility per dinuclear unit) *vs.* T plots, are shown in Fig. 14 in a temperature range 2–300 K. The $\chi_m T$ values at 300 K, 0.828 emu K mol^{-1} ($\mu_{eff} = 2.57\ \mu_B$) for **1**, which is characteristic for two non-coupled copper(II) ions with an average g factor of 2.10 ($\chi_M T = N\mu_B{}^2 g^2/2k$). As the temperature is lowered, the $\chi_m T$ values decrease in a monotonous manner and become 0.073 emu K mol^{-1} for **1** at 2 K. The curves are typical for antiferromagnetically coupled systems; the rise of the susceptibility at low temperature is caused by paramagnetic impurities.[24–26] Without these paramagnetic impurities χ_M should tend to zero at 0 K.

For dinuclear Cu(II) complexes ($S_1 = S_2 = 1/2$), the theoretical expression of the magnetic susceptibility based on the Heisenberg Hamiltonian ($H = -2JS_1S_2$) is:

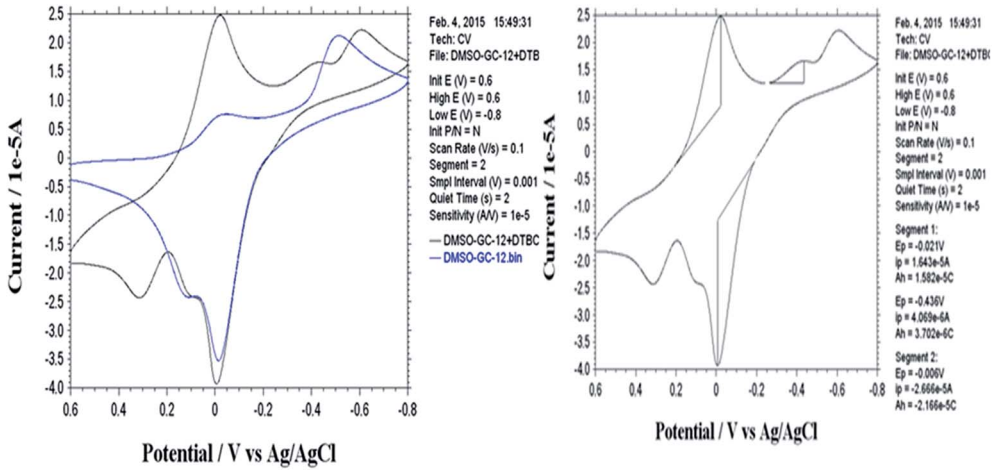

Fig. 13 CV spectrum of complex **1** after addition of 3,5-DTBC solution at the GC electrode at 100 mV s^{-1} scan rate as representative.

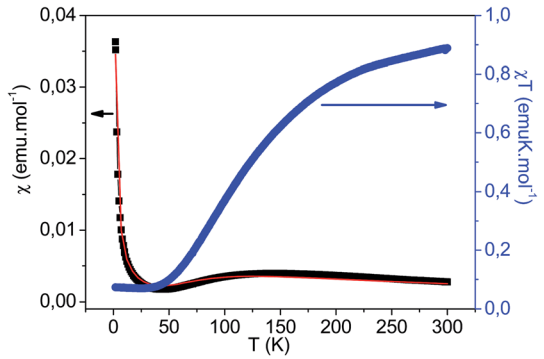

Fig. 14 Temperature variation of the magnetic susceptibilities of **1** as χ and χT *versus* T plots (the solid line represents the best fit of the experimental data based on the Heisenberg model).

$$\chi = \frac{2Ng^2\mu_B{}^2}{kT[3 + e^{-2J/kT}]}(1-\rho) + \frac{Ng^2\mu_B{}^2}{2kT}\rho + N_\alpha \qquad (1)$$

In this expression ρ present the fraction of paramagnetic impurity in the sample, N_α a temperature independent paramagnetism and the other symbols have their usual meanings. The paramagnetic impurity was assumed to be a mononuclear copper(II) species. To determine the exchange parameters, χ_M was fitted for the range 2–300 K (solid curve in Fig. 14) for **1** gives the best agreement with the experimental data for $J = -78.63 \pm 1.30$, $g = 2.13 \pm 0.03$, $\rho = 0.08 \pm 0.01$ and $N_\alpha = 0.00024 \pm 0.00008$ cm^3 mol^{-1} ($R^2 = 0.99$). The obtained magnetic parameters, J, g and ρ are compatible with the values observed for other Cu(II) dimers.[27–36]

Special characteristic feature of complex 1 in acetonitrile: dealkylation followed by oxidation to an imine ligand

An unexpected characteristic feature of this complex takes place when the synthesis of complex **1**, or its dissolution, is done in acetonitrile medium, but not in other solvents like MeOH, EtOH, DMF or DMSO. The green coloration of the solution gradually decolorizes and the color of the solution turns yellowish white. On keeping the reaction mixture for a few days white crystals suitable for X-ray diffraction were obtained. The colorless crystals are found to be $[Cu(MeCN)_4]^+$ ClO_4^- salt by X-ray analysis.[37,38] The observation reveals that discoloration is due to the reduction of Cu(II) ions to Cu(I) and the generated Cu(I) gets stabilized *via* soft–soft interaction with *N* of CH_3CN, where *N* site attains softness due to the presence of electron donating methyl group (symbiotic effect). On the other hand, solvents like MeOH, EtOH, DMF and DMSO have hard O as donor site and thereby fails to stabilize soft Cu(I) species.

Along with this reduction a concomitant oxidation should be natural consequence and it is most probably the ligand moiety which should take part in the process. In order to characterize the newly formed ligand it is essential to remove the complex as well as any unreacted metallic part which has been done according to the following manner. After complete precipitation of the Cu(I)–acetonitrile salt the remaining portion is treated with Na_2S for complete separation of copper to make the solution copper free. After filtration the yellow oil was extracted with saturated brine solution and chloroform for several times. The organic phase was separated, dried with anhydrous $MgSO_4$, concentrated by the evaporation of chloroform and subsequently vacuum-dried for the removal of last trace of water. ESI-MS study of the reaction mixture after 30 min of addition of the reactants shows a base peak at m/z 91.10 amu that may be assigned to the dealkylated fragment $PhCH_2$– (calc. $m/z = 91.126$ amu), a peak at m/z 249.10 amu corresponds to the TL species (calculated $m/z = 249.283$ amu), another peak at 327.42 corresponds to $Cu(MeCN)_4ClO_4$ (calc. $m/z = 327.202$ amu),two small peaks at m/z 434.77 due to unreacted ligand HL (calc. $m/z = 434.559$ amu) and at m/z 262.49 to unreacted copper perchlorate (calc. $m/z = 262.434$ amu). However, other peaks cannot be identified accurately. Then we perform ^1H NMR study with the purified form in D_6-DMSO medium and a sharp peak at δ 8.1 confirms the formation of an imine bond. Thereby the newly formed ligand

a Schiff-base ligand was proposed as depicted in Scheme 2. In addition the IR spectral study shows a newly generated band at 1629 cm^{-1}, previously absent in the pure HL and characteristic for a C=N bond. Our proposition has further been authenticated by ESI-MS study where a base peak observed at m/z 249.12 corresponds to the composition of the TL species (calc. m/z = 249.283 amu) along with a peak at m/z 91.51 amu as observed in earlier study.

We also monitored spectrophotometrically the whole reaction sequence. A 3 mL solution of $Cu(ClO_4)_2$ in acetonitrile is taken in quartz cell and to this solution a stoichiometric amount of the ligand HL is added and the whole course of the reaction is monitored up to 2 h at the interval of 5 min. The characteristic d–d band for Cu(II) at 600 nm gradually decreases and practically disappeared after 2 h, and this observation supports the reduction of Cu(II) to Cu(I) during the course of the reaction (Fig. 15).

To follow the transformation process we performed cyclic voltammetry study in MeCN solution. The cyclic voltammogram shows irreversible reductions at 0.065, −0.40 and −0.80 V (Fig. S29 and S30†). In DPV experiments the reductive peaks are obtained at 0.18, −0.32, −0.49 and −0.61 V. However, all these peaks in either CV or DPV experiments undergo decay with time (Fig. 16), which is consistent with the results obtained from other experiments that the complex undergoes degradation in MeCN solution. The free ligand in MeCN solution shows reductive peaks at −0.81 and −1.74 V in DPV experiments, the later peak have much stronger current height compared to the peak at less cathodic potential. On addition of $Cu(ClO_4)_2 \cdot 6H_2O$ to this solution in 2 : 1 metal : ligand ratio, the DPV undergoes dramatic change with a very strong peak appearing at −0.4 V which is characteristic of the complex and another doublet at −1.00 V and −1.14 V. The last two peaks which are neither due to the complex nor due to the original ligand may be ascribed to the reductions of the Schiff base ligand formed during degradation of the complex.

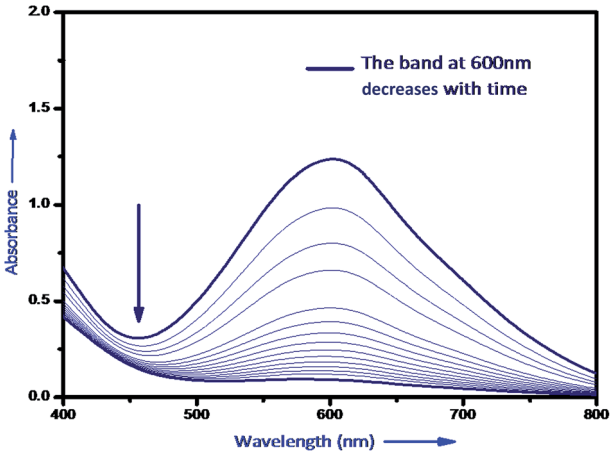

Fig. 15 The decreasing band at 600 nm during the course of reaction as the Cu(II) is converted to Cu(I).

Experimental section

Physical methods and materials

3,5-Di-*tert*-butyl catechol and (4-nitrophenyl)phosphate were purchased from Sigma-Aldrich. Reaction solutions for 3,5-DTBC and 4-NPP were prepared according to the standard sterile techniques. DMSO was dried over CaH_2 for 2 days and then distilled under reduced pressure prior to use. All other organic reagents and solvents used for synthesis were reagent grade which were obtained from commercial sources and redistilled before use. Water used in all physical measurement and experiments was Milli-Q grade.

Elemental analyses (carbon, hydrogen, and nitrogen) were performed using a Perkin-Elmer 240C analyzer. Infrared spectra (4000–400 cm^{-1}) were recorded at 28 °C on a Shimadzu FTIR-8400S and Perkin-Elmer Spectrum Express Version 1.03 using KBr pellets as mediums. ^1H and ^{13}C NMR spectra (300 MHz) were recorded in $CDCl_3$ and D_6DMSO at 25 °C on a Bruker AV300 Supercon NMR spectrometer using the solvent signal as

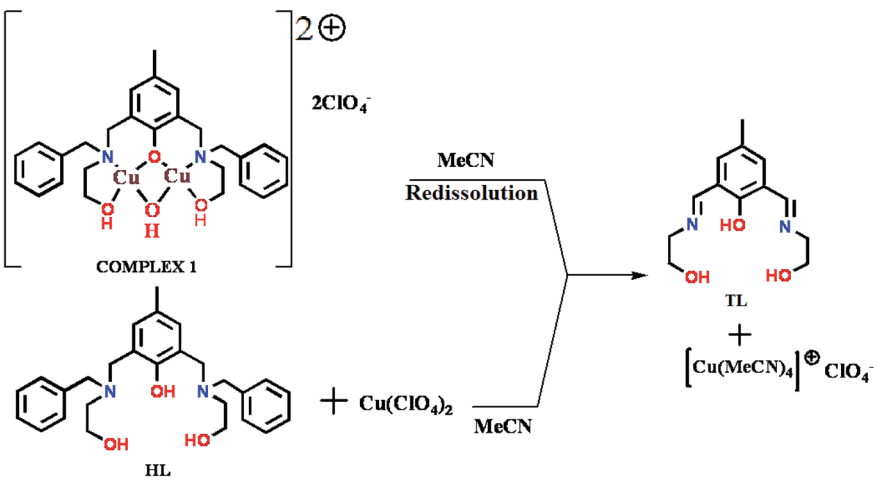

Scheme 2 Proposed scheme for the synthesis of transformed ligand TL in MeCN.

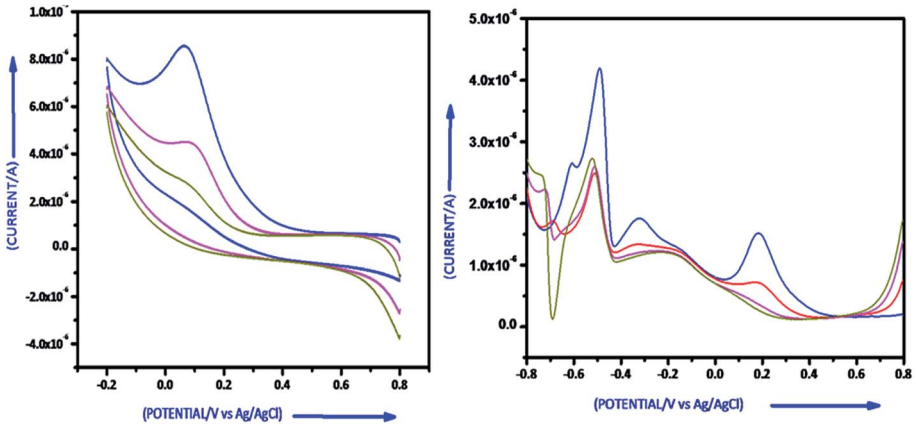

Fig. 16 Time dependent CV and DPV spectrum of complex **1** at the GC electrode in acetonitrile medium at 100 mV s^{-1} scan rate as representative.

the internal standard in a 5 mm BBO probe. UV-visible spectra and kinetic traces were monitored with a Shimadzu UV-2450PC spectrophotometer equipped with multiple cell-holders and thermostat. Magnetic susceptibility measurements over the temperature range 2–300 K were performed at a magnetic field of 0.0750 T using a Quantum Design SQUID MPMSXL-5 magnetometer. Correction for the sample holder, as well as the diamagnetic correction, which was estimated from the Pascal constants[39,40] was done. Electrospray mass spectra were recorded on a MICROMASS Q-TOF mass spectrometer. Cyclic voltammetric and DPV measurements were performed by using a CH1106A potentiostat with glassy carbon (GC) as working electrode, Pt-wire as counter electrode and Ag, AgCl/sat KCl as reference electrode. All solutions were purged with dinitrogen prior to measurements.

Synthesis of ligand HL

To an ethanolic solution (30 mL) of *p*-cresol (50 mmol, 5.407 g), 2-benzyl amino ethanol (110 mmol, 16.6 g) was added dropwise with constant stirring. After 30 min, 37% (w/v) formalin solution (115 mmol, 9.3 mL) was added to it. The resulting mixture was stirred for an additional 1 h at room temperature and then refluxed for 72 h. It was evaporated under reduced pressure, and the yellow oil was extracted with saturated brine solution and diethyl-ether for several times. The organic phase was separated, dried with anhydrous $MgSO_4$, concentrated by evaporation of ether and subsequently vacuum-dried for the removal of last traces of water. The liquid ligand was further purified by flash column chromatography (silica gel, hexane : ethylacetate : triethylamine = 100 : 5 : 1) to afford the desired β-aminophenol. Yield = 8.68 g (40%). Anal. calcd for $C_{27}H_{34}N_2O_3$: C (74.64%); H (7.83%); N (6.45%); O (11.05%); found C (75.99%); H (7.75%); N (6.80%); O (11.18%); ^{1}H NMR (300 MHz, $CDCl_3$, 25 °C): δ = 2.242 (s, 3H; ph-CH_3), ~2.7 (t, 4H; N–CH_2–CH_2), ~3.7 (t, 4H; N–CH_2–CH_2), ~3.8 (s, 4H; ph-CH_2–N), 4.37 (s, 2H; CH_2–CH_2–OH), ~6.9 (s, 2H; Ar), ~(7.22–7.35) (m, 10H; Ar); ^{13}C NMR (300 MHz, $CDCl_3$, 25 °C): δ = 20.52 (1C, ph-Me), 58.65 (2C, Ar–CH_2–N), 51.90 (2C, ph-CH_2–N), 63.32 (2C, N–CH_2–CH_2), 86.40 (2C, N–CH_2–CH_2), 116.01 (1C, Ar), 127.50 (2C, Ar), 129.39 (2C, Ar),127.49–127.86(4C–Ar), 155.18 (1C, Ar–OH); IR data (NaCl plate): ν bar = 1602, 1361, 1498, 1256, 824, 734 cm^{-1}; UV/vis (DMSO): $\lambda_{max}(\varepsilon)$ = 282.43(6840 L mol^{-1} cm^{-1}).

Synthesis of the complex $[Cu_2(L)(\mu\text{-}OH)(H_2O)(ClO_4)_2]$ (1)

To a methanolic solution (25 mL) of HL (0.5 mmol, 0.217 g), a methanolic solution (10 mL) of copper perchlorate (0.5 mmol, 0.18 g) was added and the resulting mixture was stirred for 15 min. The solution thus obtained was then filtered and the filtrate was kept in a $CaCl_2$ desiccator. After 1 day solid green product were obtained. The product was then dissolved in ethanol and after 1 week green needle shaped single crystals suitable for X-ray analysis were obtained (yield 70%). Anal. calcd for $C_{27}H_{34}Cu_2N_2O_7Cl_2$: C (46.55%); H (4.8%); N (4.02%); found: C (46.94%); H (4.89%); N (4.1%); FT-IR data (KBr pellet): I.R: ν(C–N) 1576 cm^{-1}; ν(skeletal vibration) 1496 cm^{-1}; $\nu(ClO_4)$ 1078 cm^{-1}; $\nu(ClO_4$ coordinated) 674 cm^{-1}. UV/vis (DMSO): $\lambda_{max}(\varepsilon)$ = 279(3560), 300(3520), 704 nm (120 L mol^{-1} cm^{-1}).

X-ray data collection and structure determination

Data collection of the structure reported was carried out on a Bruker Smart CCD diffractometer equipped with graphite-monochromated Mo-Kα radiation (λ = 0.71073 Å) at room temperature. Cell refinement, indexing and scaling of the data set were carried out using Bruker Smart Apex and Bruker Saint packages.[41] The structure was solved by direct methods and subsequent Fourier analyses[42] and refined by the full-matrix least-squares method based on F^2 with all observed reflections.[42] A perchlorate anion was found disordered by rotation about the Cl2–O10 bond (oxygen atoms O11/O12/O13 refined at two positions with occupancies 0.48(4)/0.52(4)). Two residuals were interpreted as a disordered lattice water molecule occupancy refined at 0.35(5)/0.65(5). All the calculations were performed using the WinGX System, Ver 1.80.05.[43] Pertinent crystallographic data and refinement details are summarized in Table 4.

Table 4 Crystallographic data and refinement details of complex 1

Empirical formula	$C_{27}H_{38}Cl_2Cu_2N_2O_{14}$	$F(000)$	1672
Formula weight	812.57	θ_{max} (°)	23.23°
Crystal system	Monoclinic	Refins collected	4388
Space group	$P2_1/n$	Unique reflections	3842
a (Å)	16.6577(14)	R_{int}	0.0531
b (Å)	14.6519(14	Observed $I > 2\sigma(I)$	2944
c (Å)	16.6876(14)	Parameters	452
β (°)	118.176(2)°	Goodness of fit (F^2)	1.2020
Volume (Å^3)	3590.3(6)	R_1 ($I > 2\sigma(I)$)	0.0834
Z	4	wR_2	0.2285
D_{calcd} (g cm^{-3})	1.503	$\Delta\rho$ (e Å^{-3})	−0.574, 0.636

Conclusion

A di-copper(II) complex of a Mannich base ligand HL has been synthesized and structurally characterized with the aim to explore its bio-relevant catalytic promiscuity by exploiting the solubility of the complex in water. X-ray structural analysis reveals that the complex resembles the active site of the catechol oxidase to a great extent having close comparable Cu–Cu separation of 2.9 Å as in the enzyme. The present complex shows interesting properties not only as catechol oxidase mimic in oxidation of 3,5-DTBC and pH dependent phosphatase-like activity, but it also reveals antiferromagnetically coupled copper centers at low temperature. To the best of our knowledge the present study represents the most suitable bio-relevant catalyst behavior reported till date in DMSO/water solvent mixture. In addition a surprising feature was observed when the complex is dissolved (or synthesized) in acetonitrile. In fact it was observed that the reduction of Cu(II) to Cu(I) (monitored by electrochemical analysis) is accompanied with dealkylation followed by concomitant oxidation of the ligand (HL) that resulted a Schiff-base species, 2,6-bis-[(2-hydroxy-ethylimino)-methyl]-4-methylphenol.

Acknowledgements

The authors wish to thank University of Calcutta for providing the facility of the single-crystal X-ray diffractometer from the DST FIST program. I.M is thankful to UGC [UGC/729/Jr Fellow(Sc)] for providing fellowship.

References

1 N. A. Rey, A. Neves, A. J. Bortoluzzi, C. T. Pich and H. Terenzi, *Inorg. Chem.*, 2007, **46**, 348.
2 R. E. H. M. B. Osorio, R. A. Peralta, A. J. Bortoluzzi, V. R. de Almeida, B. Szpoganicz, F. L. Fischer, H. Terenzi, A. S. Mangrich, K. M. Mantovani, D. E. C. Ferreira, W. R. Rocha, W. Haase, Z. Tomkowicz, A. dos Anjos and A. Neves, *Inorg. Chem.*, 2012, **51**, 1569.
3 P. J. O'Brien and D. Herschlag, *Chem. Biol.*, 1999, **6**, 91.
4 K. D. Karlin and Z. Tyeklar, *Bioinorganic Chemistry of Copper*, Chapman & Hill, New York, 1993.
5 K. S. Banu, T. Chattopadhyay, A. Banerjee, S. Bhattacharya, E. Suresh, M. Nethaji, E. Zangrando and D. Das, *Inorg. Chem.*, 2008, **47**, 7083.
6 C. Belle, C. Beguin, I. Gautier-Luneau, S. Hamman, C. Philouze, J. L. Pierre, F. Thomas and S. Torelli, *Inorg. Chem.*, 2002, **41**, 479.
7 P. Chakraborty, J. Adhikary, B. Ghosh, R. Sanyal, S. K. Chattopadhyay, A. Bauzá, A. Frontera, E. Zangrando and D. Das, *Inorg. Chem.*, 2014, **53**, 8257.
8 (*a*) R. Sanyal, A. Guha, T. Ghosh, T. K. Mondal, E. Zangrando and D. Das, *Inorg. Chem.*, 2014, **53**, 85; (*b*) R. Sanyal, X. Zhang, P. Kundu, T. Chattopadhyay, C. Zhao, F. A. Mautner and D. Das, *Inorg. Chem.*, 2015, **54**, 2315.
9 J. E. Coleman, *Annu. Rev. Biophys. Biomol. Struct.*, 1992, **21**, 441.
10 R. Sanyal, S. K. Dash, S. Das, S. Chattopadhyay, S. Roy and D. Das, *J. Biol. Inorg. Chem.*, 2014, **19**, 1099.
11 K. Nakamoto, *Infrared and Raman Spectra of Inorganic and Coordination Compounds*, John Wiley & Sons, New York, 5th edn, 1997, pp. 82–83.
12 A. Neves, L. M. Rossi, A. J. Bortoluzzi, B. Szpoganicz, C. Wiezbicki and E. Schwingel, *Inorg. Chem.*, 2002, **41**, 1788.
13 C. Fernandes, A. Neves, A. J. Bortoluzzi, A. S. Mangrich, E. Rentschler, B. Szpoganicz and E. Schwingel, *Inorg. Chim. Acta*, 2001, **320**, 12.
14 M. G. Gichinga and S. Striegler, *J. Am. Chem. Soc.*, 2008, **130**, 5150.
15 S. Torelli, C. Belle, S. Hamman and J.-L. Pierre, *Inorg. Chem.*, 2002, **41**, 3983.
16 (*a*) J. Reim and B. Krebs, *J. Chem. Soc., Dalton Trans.*, 1997, 3793; (*b*) C. Gerdemann, C. Eicken and B. Krebs, *Acc. Chem. Res.*, 2002, **35**, 183.
17 (*a*) E. I. Solomon, U. M. Sundaram and T. E. Machonkin, *Chem. Rev.*, 1996, **96**, 2563; (*b*) J. Mukherjee and R. Mukherjee, *Inorg. Chim. Acta*, 2002, **337**, 429; (*c*) S. Mandal, J. Mukherjee, F. Lloret and R. Mukherjee, *Inorg. Chem.*, 2012, **51**, 13148.
18 (*a*) M. R. Mendoza-Quijano, G. Ferrer-Sueta, M. Flores-Álamo, N. A. Alcalde, V. Gómez-Vidales, V. M. Ugalde-Saldívara and L. Gasque, *Dalton Trans.*, 2012, 4985; (*b*) A. Biswas, L. K. Das, M. G. B. Drew, C. Diaz and A. Ghosh, *Inorg. Chem.*, 2012, **51**, 10111.
19 V. R. deAlmeida, F. R. Xavier, R. E. H. M. B. Osório, L. M. Bessa, E. L. Schilling, T. G. Costa, T. Bortolotto, A. Cavalett, F. A. V. Castro, F. Vilhena, O. C. Alves, H. Terenzi, E. C. A. Eleutherio, M. D. Pereira, W. Haase, Z. Tomkowicz, B. Szpoganicz, A. J. Bortoluzzi and A. Neves, *Dalton Trans.*, 2013, 7059.
20 L. J. Daumann, P. Comba, J. A. Larrabee, G. Schenk, R. Stranger, G. Cavigliasso and R. Gahan, *Inorg. Chem.*, 2013, **52**, 2029.
21 M. Lanznaster, A. Neves, A. J. Bortoluzzi, B. Szpoganicz and E. Schwingel, *Inorg. Chem.*, 2002, **41**, 5641.
22 V. K. Bhardwaj and A. Singh, *Inorg. Chem.*, 2014, **53**, 10731.
23 S. Bosch, P. Comba, L. R. Gahan and G. Schenk, *Inorg. Chem.*, 2014, **53**, 9036.

24 R. Prabu, A. Vijayaraj, R. Suresh, L. Jagadish, V. Kaviyarasan and V. Narayanan, *Bull. Korean Chem. Soc.*, 2011, **32**, 1669.
25 J. Mrozinski, *Coord. Chem. Rev.*, 2005, **249**, 2534.
26 S. S. Tandon, V. Bunge, D. Motry, J. S. Costa, G. Aromi, J. Reedijk and L. K. Thompson, *Inorg. Chem.*, 2009, **48**, 4873.
27 Y. Song, D.-R. Zhu, K.-L. Zhang, Y. Xu, C.-Y. Duan and X.-Z. You, *Polyhedron*, 2000, **19**, 1461.
28 F. Bentiss, M. Lagrenee, O. Mentre, P. Conflant, H. Vezin, J. P. Wignacourt and E. M. Holt, *Inorg. Chem.*, 2004, **43**, 1865.
29 A. Ali, S. Salunke-Gawali, C. P. Rao and J. Linares, *Indian J. Chem., Sect. A: Inorg., Bio-inorg., Phys., Theor. Anal. Chem.*, 2006, **45**, 853.
30 A. Banerjee, R. Singh, E. Colacio and K. K. Rajak, *Eur. J. Inorg. Chem.*, 2009, 277.
31 P. Cheng, D. Liao, S. Yan, Z. Jiang, G. Wang, X. Yao and H. Wang, *Inorg. Chim. Acta*, 1996, **248**, 135.
32 T. Mallah, O. Kahn, J. Gouteron, S. Jeannin, Y. Jeannin and C. J. O'Connorl, *Inorg. Chem.*, 1987, **26**, 1375.
33 T. Chattopadhyay, K. S. Banu, A. Banerjee, J. Ribas, A. Majee, M. Nethaji and D. Das, *J. Mol. Struct.*, 2007, **833**, 13.
34 S. Sarkar, S. Majumder, S. Sasmal, L. Carrella, E. Rentschler and S. Mohanta, *Polyhedron*, 2013, **50**, 270.
35 A. Benzekri, P. Dubourdeaux, J. M. Latour, J. Laugier and P. Rey, *Inorg. Chem.*, 1988, **27**, 3710.
36 O. Kahn, T. Mallah, J. Gouteron, S. Jeannin and Y. Jeannin, *J. Chem. Soc., Dalton Trans.*, 1989, 1117.
37 M. Stanley, E. Reynold and T. Iwamoto, *J. Electroanal. Chem.*, 1967, **14**, 213.
38 G. Rainoni and A. D. Zuberbuehler, *Chimia*, 1974, **28**(2), 67.
39 C. J. O'Connor, *Prog. Inorg. Chem.*, 1982, **29**, 203.
40 G. A. Bain and J. F. Berry, *J. Chem. Educ.*, 2008, **85**, 532.
41 *SMART, SAINT, Software Reference Manual*, Bruker AXS Inc., Madison, WI, 2000.
42 G. M. Sheldrick, *Acta Crystallogr., Sect. A: Found. Crystallogr.*, 2008, **64**, 112.
43 L. J. Farrugia, *J. Appl. Crystallogr.*, 2012, **45**, 849.